Research Article | Vol. 12, No. 7 / 1 July 2021 / Biomedical Optics Express 4235
Biomedical Optics EXPRESS

Microvascular blood flow changes of the abductor pollicis brevis muscle during sustained static exercise

MARTINA GIOVANNELLA,[1] EVELINA URTANE,[2] MARTA ZANOLETTI,[1,*] UMUT KARADENIZ,[1] ULDIS RUBINS,[3] UDO M. WEIGEL,[4] ZBIGNEVS MARCINKEVICS,[2] AND TURGUT DURDURAN[1,5]

[1]*ICFO-Institut de Ciències Fotòniques, The Barcelona Institute of Science and Technology, 08860 Castelldefels (Barcelona), Spain*
[2]*Faculty of Biology, Department of Human and Animal Physiology, University of Latvia, Kronvalda Blvd. 4, LV 1586, Riga, Latvia*
[3]*Institute of Atomic Physics and Spectroscopy, University of Latvia, 19 Rainis Blvd., Riga LV- 1586, Latvia*
[4]*HemoPhotonics S.L., Av. Carl Friedrich Gauss Num. 3, 08860 Castelldefels (Barcelona), Spain*
[5]*Institució Catalana de Recerca i Estudis Avançats (ICREA), 08010 Barcelona, Spain*
[*]*marta.zanoletti@icfo.eu*

Abstract: A practical assessment of the general health and microvascular function of the palm muscle, abductor pollicis brevis (APB), is important for the diagnosis of different conditions. In this study, we have developed a protocol and a probe to study microvascular blood flow using near-infrared diffuse correlation spectroscopy (DCS) in APB during and after thumb abduction at 55% of maximum voluntary contraction (MVC). Near-infrared time resolved spectroscopy (TRS) was also used to characterize the baseline optical and hemodynamic properties. Thirteen (n=13) subjects were enrolled and subdivided in low MVC (N=6, MVC<2.3 kg) and high MVC (N=7, MVC≥2.3 kg) groups. After ruling out significant changes in the systemic physiology that influence the muscle hemodynamics, we have observed that the high MVC group showed a 56% and 36% decrease in the blood flow during exercise, with respect to baseline, in the long and short source-detector (SD) separations (p=0.031 for both). No statistical differences were shown for the low MVC group (p=1 for short and p=0.15 for long SD). These results suggest that the mechanical occlusion, due to increased intramuscular pressure, exceeded the vasodilation elicited by the higher metabolic demand. Also, blood flow changes during thumb contraction negatively correlated (R=-0.7, p<0.01) with the absolute force applied by each subject. Furthermore, after the exercise, muscular blood flow increased significantly immediately after thumb contractions in both high and low MVC groups, with respect to the recorded values during the exercise (p=0.031). An increase of 251% (200%) was found for the long (short) SD in the low MVC group. The high MVC groups showed a significant 90% increase in blood flow only after 80 s from the start of the protocol. For both low and high MVC groups, blood flow recovered to baseline values within 160 s from starting the exercise. In conclusion, DCS allows the study of the response of a small muscle to static exercise and can be potentially used in multiple clinical conditions scenarios for assessing microvascular health.

1. Introduction

The metabolic demand of skeletal muscles increases during exercise and the assurance of proper blood perfusion is fundamental for the muscle well-being. However, it can be compromised in various pathological conditions [1–4]. In particular, small palmar muscles are often compromised by daily manipulations such as heavy computer usage and extensive manipulation of a hand-held

#427885 https://doi.org/10.1364/BOE.427885
Journal © 2021 Received 20 Apr 2021; revised 9 Jun 2021; accepted 9 Jun 2021; published 18 Jun 2021

Biomedical Optics EXPRESS

device [5]. The continuous overuse of small palm muscles that control fine movements of the thumb (thenar muscles) creates damage and inflammation resulting in the stiffening and pain in the thenar eminence (soft muscular rounded part at the base of the thumb) causing the so called repetitive strain injury.

Of particular interest is the assessment of blood perfusion to this area as an indicator of proper thenar muscle function. This work focuses on the abductor pollicis brevis (APB) that is the most lateral and superficial of the three muscles forming the thenar eminence and it is a flat, thin, triangular fusiform muscle. It is the smallest intrinsic thenar muscle and one of the few intrinsic muscles innervated by the median nerve with the large number of small motor units [6,7]. APB's main function is to move the thumb away from the palm in a direction perpendicular to the surface of the palm itself (palmar abduction) [8–10] and it is essential for proper hand functioning [11]. Its health and function can be compromised by conditions such as the carpal tunnel syndrome (CTS) [12] which can cause it to weaken and atrophy [13]. Interestingly, it has been shown that the assessment of the atrophy and the strength of the APB during exercise can be useful for CTS diagnosis [14] and can predict the failure or success of surgical treatment [15]. In addition, vascular changes have been proven to precede electrophysiological abnormalities in patients with evidence of CTS [16].

To date, the blood perfusion to the thenar muscles has only been monitored by means of Doppler ultrasonography in the forearm [17,18] which provides information from the large vessels that irrigate more than one muscle. Better and practical methods are still needed to evaluate local, specific biomarkers for impaired blood perfusion. With this purpose, various methods have been explored to measure blood perfusion in exercising skeletal muscle [4] but none of them are satisfactory for measuring the local muscle blood flow. Among the cost-effective, non-invasive, continuous and easily available options, laser Doppler flowmetry [19] and venous occlusion plethysmography [20] are promising. The former is restricted to shallow (< 1 mm) tissue measurements, while the latter requires interruption of venous blood flow, limiting the clinical scenarios it can be applied to.

Near-infrared spectroscopy (NIRS) based technologies are good candidates for monitoring the hemodynamics of skeletal muscle thanks to their non-invasiveness and cost-effectiveness [21]. Typical NIRS can measure microvascular blood oxygen saturation dynamics [22,23]. Recently, another technique using near-infrared but coherent light has been emerging for this purpose, i.e. diffuse correlation spectroscopy (DCS) [24–26], which can measure microvascular blood flow in deep (~1 cm) tissues. DCS has already been validated for muscle blood flow measurements [27] and has been exploited to measure perfusion of large skeletal muscles (*e.g.* leg, thigh and forearm) mainly during dynamic exercise protocols [28].

The aim of this study is first to characterize the APB resting state and hemodynamics, then to assess blood flow in APB using DCS. We utilize a static exercise which strongly challenges the APB muscle and can lead to blood flow changes depending on the muscle contraction force, muscle shape and thickness. We have selected a static exercise of moderate intensity in order to minimize any systemic response that depends on the muscle volume and exercise intensity [29,30]. Therefore, the results presented here reflect the local perfusion response to the exercise and its evolution during post-exercise recovery.

2. Methods

2.1. Diffuse optical monitors for muscle hemodynamics and data analysis

DCS measures the intensity fluctuations of a single speckle resulting from the propagation through the tissue of long coherence length NIR laser light. Intensity fluctuations are affected by the movement of scatterers present in the tissue, dominated by the red blood cells [24]. By studying the decay of the intensity autocorrelation function a measure of the Brownian diffusion coefficient (D_B) of moving scatterers can be retrieved [25]. In tissues, D_B weighed by the ratio of

Biomedical Optics EXPRESS

the moving to static scatterers has been shown to be a reliable blood flow index (BFI) which is proportional to local, microvascular blood flow [26,31] and it is measured in cm^2/s. We have measured BFI using a commercial DCS device (HemoFloMo, HemoPhotonics S.L., Spain). The device uses a continuous wave long coherence length laser operating at 785 nm and it has four parallel source channels and eight parallel detector channels. For the scope of this study, only one of the source and two of the detector channels were used. The probe we have developed consists of a black foam material embedding one source and two detection fibers at 8 mm and 15 mm far from the source (refer to Fig. 1) which we refer to as the short and long source-detector (SD) separations. DCS measurements were analyzed using the solution for the diffusion equation for the electric field autocorrelation function in a semi-infinite medium [25,26] to derive the BFI.

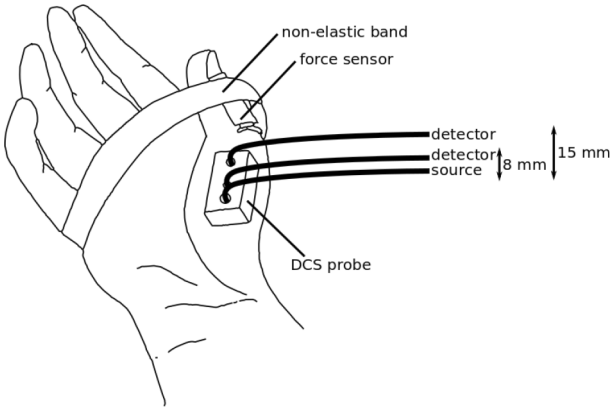

Fig. 1. The placement of the DCS probe on the APB muscle. One detector fiber was kept at a distance of 8 mm, while the other was at 15 mm from the source fiber. The thumb was kept attached to the hand by a non-elastic band, which held a force transducer in order to measure the strength applied toward the band by the thumb. Subject's hands were placed on a vacuum pillow support to avoid movement (not shown in the figure).

In addition to DCS, near-infrared time resolved spectroscopy (TRS) was exploited for obtaining the optical properties of the APB muscle using a commercial prototype dual-channel TRS device (TRS-20, Hamamatsu Photonics K.K, Japan). This device employs NIR laser pulses of hundreds ps at 760 nm, 800 nm and 830 nm. The combination of the two systems and the data analysis were previously explained [32]. The backscattered photon time of flights were collected from the channel with 15 mm source-detector (SD) separation separately from DCS data. Finally, TRS curves were then fitted to the time dependent analytical solution of the diffusion equation for semi-infinite homogeneous medium in order to retrieve the absorption (μ_a) and reduced scattering ($\mu_s\prime$) characterizing the probed tissue [33,34]. Optical properties measured by the TRS at 800 nm were used for the DCS analysis as input parameters [35]. This approach allowed us to characterize the resting state hemodynamics prior to moving onto the dynamic scenario.

2.2. Protocol

Healthy, right-handed adult subjects were recruited for a single measurement session. The study was approved by the ethical committee of Hospital Clinic Barcelona (Spain). Each subject signed an informed consent and the study was conducted according to the principles of the Declaration of Helsinki.

The subject was seated on a comfortable reclined chair with the right hand lying on a vacuum pillow adapted to the hand shape to avoid movement and to keep the hand at heart level. The area occupied by the APB muscle was highlighted by an ultrasound (US) in brightness mode

Biomedical Optics EXPRESS

(Sonosite Titan L38 transducer, UMI, US). An US image was acquired for each subject in order to calculate the thickness of skin, adipose tissue and muscle layer. US measurements were carried out to investigate the role of the adipose tissue thickness as a confounding factor. The use of a layered tissue model for data analysis is beyond the scope of this work.

A measurement of thirty seconds was performed by placing the TRS probe on the APB location, which was then used to estimate its μ_a and $\mu_s\prime$. Afterwards, the DCS probe was attached carefully on the same area. A force transducer (Flexi Forxe Sensor III, Tekscan, US) was kept on the external part of the thumb by a non-elastic band placed over the hand to avoid movements of the thumb (Fig. 1). The force measured as a voltage by the force sensor was calibrated by pressing the sensor over a scale resulting in a conversion factor of 1.3 kg/V. A screen (Gauge Indicator, LabVIEW, US) displayed the reading of the force sensor on-line. Once the DCS probe, the force transducer and the band were appropriately placed, the maximum voluntary contraction (MVC) was measured. In order to measure the MVC, the subject was asked to press the thumb against the non-elastic band for at least five seconds. The process was repeated three times and the average recording used as the MVC.

At this point, DCS acquisition was started. After three minutes of rest, the subject was asked to press the thumb towards the belt applying 55% of the MVC and maintain its pressure constant for thirty seconds following the force sensor recording displayed on the screen.

Afterwards the subject rested for three minutes and another thirty seconds of exercise at 55% of the MVC followed. Similar to the first exercise, three minutes of rest were measured after the second exercise. DCS measurements were acquired at 1 s averaging time, but the acquisition was paused for 5 s after every five acquired curves in order to record acquisitions by another device which is not related to this study.

During the whole protocol, the mean arterial pressure (MAP), the heart rate (HR) and the cardiac output (CO) were measured on the non-exercising hand, by a non invasive continuous blood pressure monitor (Finometer Midi, Finapres, Netherlands).

2.3. Statistical data analysis

At first, median, first and third interquartile values were calculated for layer thicknesses, MVC, optical properties, baseline BFI and baseline physiological parameters (MAP, CO, HR). In particular, the baseline period was defined as the 60 s before starting each exercise (*i.e.* the calculation of changes with respect to baseline was done independently for each exercise repetition). BFI was finally normalized to the baseline to derive a relative BFI (rBFI) and a rBFI percentage change (ΔrBFI). It is worth noting that DCS measurements that were acquired right before and right after the exercise were excluded to rule out motion artifacts.

In order to characterize the response to exercise, the change of physiological parameters and ΔrBFI was evaluated for each subject in four time windows. The start time point of the exercise was marked as t=0 s. Then, time windows were defined as follow: (1) “During” from t=15 s to t=30 s, during the exercise; (2) “Post1”, at t=40±5 s; (3) “Post2” at t=80±5 s, and, (4) “Post3” at t=160±5 s, after the exercise.“Post1” was chosen to reflect the time interval right after the exercise where the largest hemodynamic response occurs.

Since the goal was to study the response of the local microvascular blood perfusion in the muscle to the exercise, and to avoid data contamination by systemic changes, we have tested whether CO, MAP and HR changed during and after exercise. All the three parameters were evaluated in each of the four temporal windows aforementioned for each exercise repetition by using a Wilcoxon signed-rank test. In addition, a paired Wilcoxon signed-rank test was run between “During” and “Post1”, "Post2" and “Post3” time points, in order to test whether there is a further change after the end of the exercise. No corrections were applied for multiple comparisons. In order to compare results obtained right after the exercise ("Post1") between the low MVC and high MVC group, we also performed a Mann-Whitney U test. Finally, the

Biomedical Optics EXPRESS

response of microvascular blood flow to exercise was evaluated. First, we have tested whether the two exercise repetitions triggered a different response. To do so, a linear mixed effect (LME) model was built with the exercise repetition as the fixed effect and the subject identifier as the random effect for each of the four selected time windows and source-detector separations.

To conclude with, we have aimed to check if the change in blood flow during and after exercise depends on the absolute force applied by each subject, whose MVC is a surrogate measure. Therefore, a correlation between ΔrBFI in the four time-windows and the MVC was tested through calculation of the Pearson coefficient (R). The Pearson coefficient was used also to investigate the correlation between MVC and the measured layer thickness by the US. Statistical data analysis was performed through R [36] and MATLAB (Statistics Toolbox Release 2020b, The MathWorks, Inc., US). Threshold for significance was set for p-values < 0.05 for all statistical tests.

3. Results

Thirteen subjects (n=13) were recruited for the study. An example of an ultrasound image is shown in Fig. 2(a). The thicknesses of the skin, adipose subcutaneous tissue and muscle layer are shown in Fig. 2(b) for each subject. The median of the superficial layer thickness (skin and adipose tissue layer) was 2.1 mm (1.7 mm, 2.4 mm). The first and third interquartile are shown in brackets throughout the rest of the text. The median thickness of APB muscle was 6.3 mm (5.2 mm, 7.6 mm).

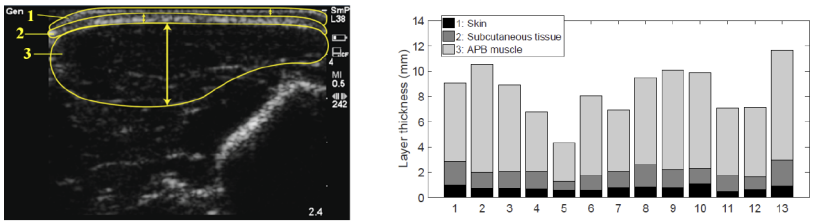

(a) (b)

Fig. 2. (a) An ultrasound image acquired from one subject. Three different structures can be defined: the skin (1), the adipose subcutaneous tissue (2) and the abductor pollicis brevis (APB) muscle (3). (b) The three layer thicknesses measured in all the subjects. The skin and adipose subcutaneous tissues are referred as the superficial layer for the rest of the manuscript.

The MVC measured for each subject and a summary boxplot is reported in Fig. 3(a) and (b). Interestingly, there is a heterogeneous distribution of the results with a median of 2.3 kg (1.9 kg, 2.9 kg). Given this result, we have decided to divide the subjects into two groups (high and low MVC) which is purely based on the division observed in this study and does not imply a physiological differentiation. Here, the median, represented by a black dashed line in the Fig. (upper panel), divides the subjects into two groups: (i) low MVC (N=7, MVC<2.3 kg) and (ii) high MVC (N=6, MVC≥2.3 kg) group. We did not find a correlation between the MVC and the muscle layer thickness as measured by the US (R=-0.073 and p=0.81).

The baseline values for physiological parameters, optical properties and BFI are summarized in Table 1. Furthermore, the optical properties and BFI are reported for each subject in Fig. 4. MAP did not change during the two exercises (p=0.46 and p=0.10 for first and second exercise respectively). Same results were obtained for changes in HR (p=0.32) and CO (p=0.083) in the first exercise. On the other hand, a small increase was registered for HR and CO in the second part of the protocol. In fact, HR increased by 3.5 bpm (5% of the baseline, p=0.007) and CO by 0.5 L/min (7% of the baseline, p=0.002).

Biomedical Optics EXPRESS

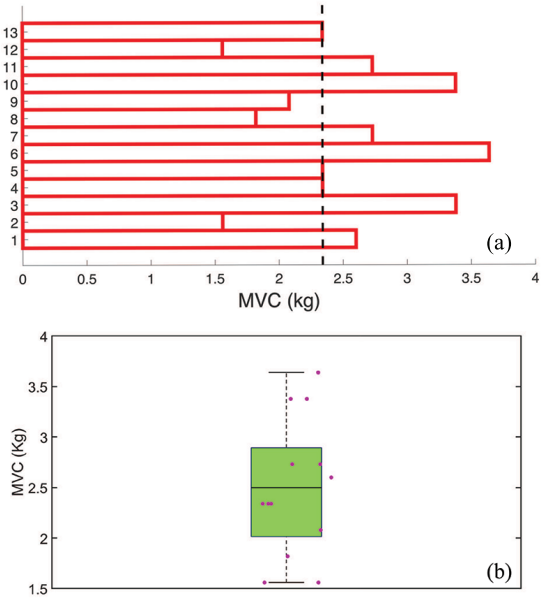

Fig. 3. MVC measured in the 13 subjects. Median (first, third interquartile) is 2.3 kg (1.9 kg, 2.9 kg). The black vertical line in (a) corresponds to the median value. The summary boxplot in (b) highlights the heterogeneity of the MVC that leads into the separation of subjects into two different groups. Here, the boxplot shows the mean, 25th and 75th percentiles with the whiskers showing the extreme non-outlier points.

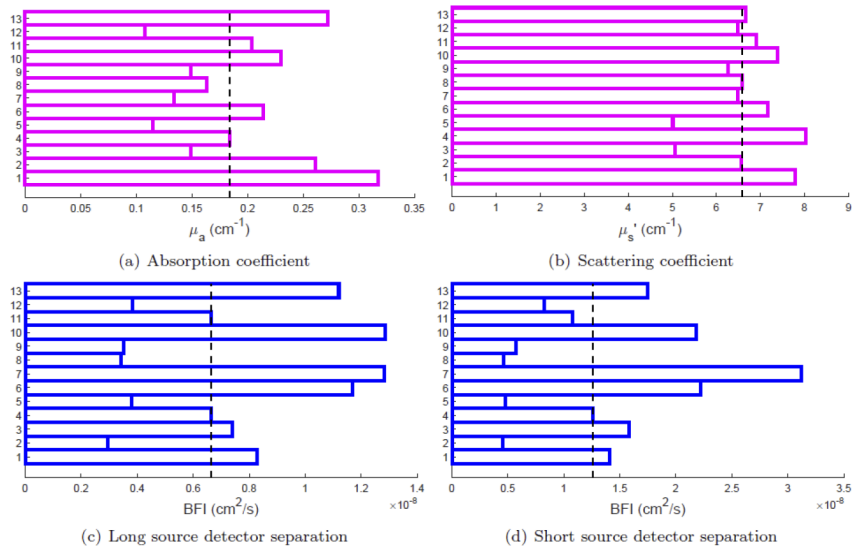

Fig. 4. Optical properties at 800 nm (n=13) by TRS showing (a) absorption and (b) reduced scattering coefficient. BFI measured by DCS from the long (c) and short (d) source-detector separations. The dashed vertical line represents the median. First and third interquartile are reported in Table 1.

Biomedical Optics EXPRESS

Table 1. Median (first, third interquartile) of baseline values over all the subjects (n=13). Mean arterial pressure (MAP), heart rate (HR), cardiac output (CO), absorption (μ_a) and reduced scattering coefficient (μ_s') at 800 nm, and blood flow index (BFI) are reported.

Physiological parameters	
MAP	88 (84,98) mmHg
HR	67 (62,77) bpm
CO	7.0 (5.3,8.6) L/min
Optical properties @800 nm	
μ_a	0.18 (0.14, 0.24) cm^{-1}
μ_s'	6.6 (6.4, 7.22) cm^{-1}
Blood flow index (BFI)	
Long separation (15 mm)	0.7 (0.4, 1.4) $\times 10^{-8}$ cm^2/s
Short separation (8 mm)	1.0 (0.6, 2.2) $\times 10^{-8}$ cm^2/s

LME analysis confirmed that the BFI response was equivalent in the two exercise repetitions throughout the four time windows and for both long and short SD (p>>0.05 for all cases).

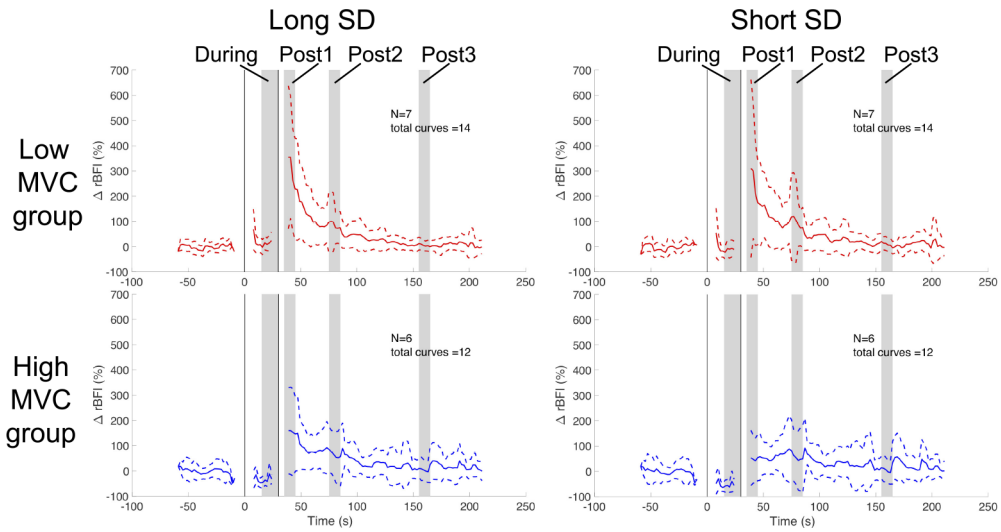

Fig. 5. ΔrBFI as measured in the APB during and after 30 s of sustained thumb abduction at 55% MVC. The start time-point of the exercise is defined at t=0 s and the vertical black lines highlight the exercise period (from 0 s to 30 s). Results from the group with low MVC (N=7) are shown in red in the upper row, while results from the group with high MVC (N=6) in blue in the bottom one. The long SD is displayed in the left column and the short in the right one. The four time windows of interest are highlighted by grey vertical areas. ΔrBFI time traces are obtained by averaging values in the two sessions of exercise for N=7 (low MVC group) and N=6 (high MVC group) subjects.

Figure 5 shows the time series of ΔrBFI for the two groups (high and low MVC) and the two DCS SD separations averaged over subjects (N=7 in low MVC group and N=6 in high MVC group) and over the two exercises. The results are summarized by boxplots in Fig. 6 for ΔrBFI calculated in the four time windows of interest, where each dot represents one subject. Stars

Biomedical Optics EXPRESS

highlight statistically significant difference with respect to the baseline ($p<0.05$) as tested by the Wilcoxon signed-rank test.

In the high MVC group, we observe a significant 36% decrease ($p=0.031$) of ΔrBFI at the long SD distance during the exercise which is similar to those obtained for the short SD distance (decrease of 56%, $p=0.031$). In the low MVC group ΔrBFI stayed similar to the baseline at both long and short SD separations ($p=1$ for short and $p=0.15$ for long SD).

In the low MVC group, right after the exercise ("Post1"), blood flow increased of 251% ($p=0.031$) and about 200% (also $p=0.03$) in long and short SD separations. On the other hand, the high MVC group did not show a significant increase during "Post1" period at either SD separations ($p=0.437$ for short and $p=0.063$ for long SD). In this specific time-window we found a statistical difference between high and low group at the short SD ($p=0.035$). No statistical difference was observed at long SD ($p=0.23$).

"Post2" period showed an increase in ΔrBFI of about 50% for both long and short SD ($p=0.016$) in the low MVC group. In this case, blood flow recovered within 160 s after the exercise for both short and long source-detector separations. In the high MVC group statistical significance was observed only by the long SD (increase of 90%, $p=0.031$ for "Post2") and the blood flow recovered within 90 s after the task.

Blue brackets in Fig. 6 highlight statistically significant changes of ΔrBFI after the exercise. Comparing "Post1"and the median values of ΔrBFI obtained during the exercise for the low MVC group, statistically significant differences are shown in both short and long SD with an increase of 188% ($p=0.031$) and 203% ($p=0.031$) respectively. In the same group, 52% higher values are shown also between "Post2" and "During" time windows ($p=0.0156$) for the short SD.

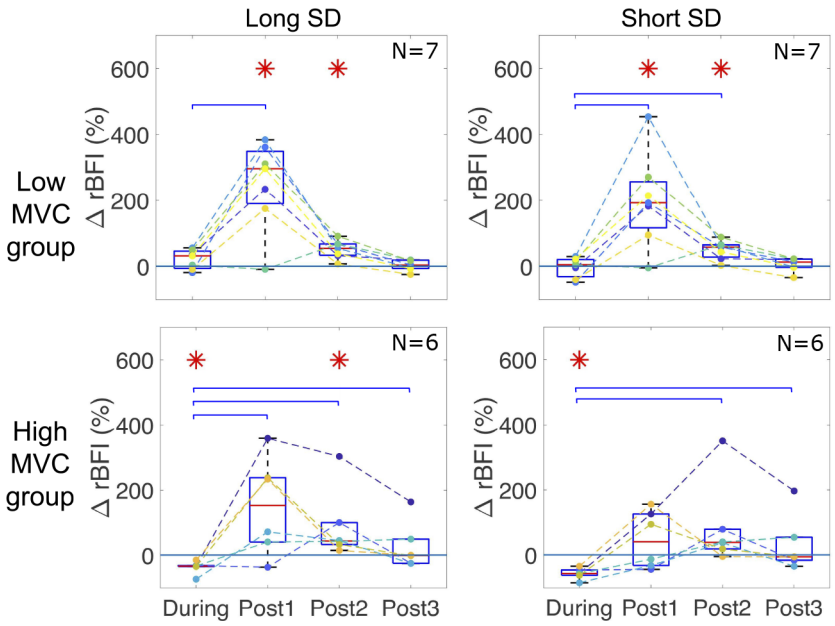

Fig. 6. Boxplots of ΔrBFI for the two source-detector separations (columns) divided according to the MVC group (rows). The four periods correspond to "During" from 15 s to 30 s, i.e. during exercise (start at 0 s) and post-exercise "Post1" at 40 s, "Post2" at 80 s and "Post3" is at 160 s. Red stars indicate statistically significant difference with respect to baseline. Blue brackets indicate statistically significant difference between "During" and the tested period. See main text for further details. Each dot overlaying the boxplots represent one subject.

Biomedical Optics EXPRESS

On the other hand, "Post3" values were not statistically different from the one retrieved during the exercise (p=0.69 for short and p=0.21 for long SD). As far as the high MVC group is concerned, a significant increase of about 229% (p=0.031), is shown in "Post1" with respect to the median value reached in the exercise window, in the long SD. No statistical differences are shown in the short SD (p=0.063). It is possible to note also higher values (144% for short and 126% long SD, p=0.031 for both) comparing "Post2" and "During" the exercise. Finally, differences hold in "Post3" temporal window with respect to the exercise for both short and long SD (p=0.031 for both) with 88% and 66% increase respectively.

Lastly, the correlation between the ΔrBFI and the MVC was tested in each of the four time windows considered. A statistically significant correlation was found only during thumb abduction both for long (R=-0.7, p=0.009) and short source-detector separation (R=-0.6, p=0.02). Other correlations were non-significant.

4. Discussion

To the best of our knowledge, this is the first time that the optical properties of the APB muscle are reported. The literature shows a wide-range for the optical properties of different skeletal muscles such as calf, vastus lateralis or forearm which may be similar. Even though there is no clear consensus in the literature about muscle optical properties, the APB optical properties reported in this work fall within the range of absorption and reduced scattering coefficients reported for the forearm. For example, in [37], a $\mu_s\prime$=6.8±0.8 cm^{-1} and μ_a=0.23±0.04 cm^{-1} on the forearm of fourteen subjects was reported. Similar results are also shown in [38]. When considering the vastus lateralis, in [39] $\mu_s\prime$=6.23±1.24 cm^{-1} and μ_a=0.26±0.06^{-1} at 828 nm are reported at the baseline which are also similar. On the calf muscle, the results are often higher with respect to the values retrieved in this study [40]. We expect our studies and others will pave the way for further studies to expand this literature.

APB is involved in important hand functions and its performance can be compromised by musculo-skeletal disorders of the upper extremities. In addition, it is a relevant muscle to consider as a model to study the microvascular blood flow dynamics that are affected by the local physiology rather than a larger reaction that alters the systemic physiology. This was hypothesized because a moderate intensity exercise of a small muscle like APB, whose total blood supply is rather limited [7], is not expected to influence the systemic circulation [29]. Our results indicate this to be true for the first period of exercise with a minimal, possibly stress induced change in the systemic physiology during the second repetition. Overall, our findings are within physiological expectations and illustrate that DCS is indeed a potential technology to further explore and adapt for understanding local muscle physiology. We now discuss specific results and limitations of the study.

The protocol and the subject population were verified to be appropriate since an indicator, MVC in each subject (Fig. 3), was found to be comparable to previously published results [10,41,42]. Also, we did not find a significant correlation between the MVC and the thickness of the muscle. Given this result, we can argue that thickness of the APB muscle is not the primary determinant factor for muscle strength as far as this study is concerned [43]. Since APB has not been studied extensively, it is not possible to derive more specific insights into the observed variation of MVC. In general, there are many other factors ranging from structural/anatomical ones to the well-being of the subject to the training levels.

In order to verify how the protocol affected systemic circulation, the heart rate (HR), mean arterial blood pressure (MAP) and cardiac output (CO) were monitored throughout the whole measurement time. In particular, MAP did not change along the whole protocol, while we have found a small increase during the second exercise for HR and CO of 3 bpm and 0.5 L/min respectively. Different reasons may have lead to this increase in the second repetition of exercise. The subject may have been more stressed during the second repetition with respect to the first

Biomedical Optics EXPRESS

one or they may have involved more muscles because they knew what to expect. The measured changes are far smaller than what was reported in moderate intensity exercises of larger muscles [30,44] and we do not expect this to influence muscle blood flow. Furthermore, the blood flow response as measured by DCS did not differ between the two exercise repetitions.

Perfusion response to sustained isometric exercise is currently not fully understood because of different factors playing roles in the process. On one hand, the metabolic demand of the muscle is higher and this leads to the release of metabolites to ensure vasodilation in the muscle of interest [45]. On the other hand, the contraction increases the intramuscular pressure and mechanically occludes the vessels in that region, partially or totally. The pressure depends on the contraction force and it has been observed that moderate intensity exercises (55% of MVC) lead to a decreased or unchanged perfusion to the muscle during the first tens of seconds of exercise [46–48]. This is different from dynamic rhythmic exercise during which muscle perfusion increases due to the relaxation period [49].

In agreement with these observations from the literature, overall, the blood flow as measured by DCS in our experiment did not increase during static exercise for the low MVC group. Interestingly, we have observed a different behavior in subjects with high MVC, who performed exercise at a stronger force, compared to the low MVC ones. In particular, muscle blood flow significantly decreased during exercise in the high MVC group with respect to the baseline. This finding suggests that the intramuscular pressure depends not only on the relative intensity with respect to the MVC but also on the absolute force that is higher in the high MVC group. This type of relationship has been previously discussed in literature [47,50].

The authors cannot exclude the possibility that high MVC group activates other muscles during the contraction that does not increase the MVC itself but could redistribute blood flow during post exercise recovery period. These mechanisms, called vascular shunt mechanisms, are complex and their study in the future can be enabled by these technologies [51]. Thus, the APB blood flow in the high MVC group decreases, largely due to compression of the pollicis muscle, and possibly due to activation of other muscles during static thumb abduction that result in shunting blood supply to the muscle during hyperaemia.

We have found a statistically significant negative correlation between the change of blood flow during exercise and the MVC measured in each subject. The higher the MVC, *i.e.* the force applied, the lower the blood flow during exercise, presumably due to the increased intramuscular pressure. This topic can be further explored using different protocols and in a larger population. After the exercise, the blood flow increased with respect to the exercise period and, for the low MVC group, it reached higher levels than baseline. This was expected due to the previously elicited vasodilation since muscle relaxation stops the mechanical occlusion. When comparing the high and low MVC group during the "Post1" interval we saw statistically different hemodynamic responses at short SD. Interestingly we did not see the same difference at longer SD. Whether this is a true finding indicating that the superficial tissues that are probed preferentially by the short SD are showing a different recovery after exercise in these two groups should further be studied.

Through the study, comparable, but not equivalent, results were registered by the long and the short source-detector separations. It must be reminded that DCS measures a mixture of extra- and intra-muscular perfusion and the weight of the former is more prominent in the short source-detector separation. These results confirm that, even if the superficial layer on top of the APB is very thin (2.1±0.5 mm), it partially masks the muscle perfusion to the detector placed at 8 mm from the source. The two separations (possibly additional ones) could have been utilized in a two-layer medium approximation to provide an even better analysis of the underlying muscle perfusion. However, we argue that given this thin superficial layer and the fact that it was feasible to use a probe with an intra-fiber distance of 15 mm both in terms of the muscle geometry and the signal intensity, the use of a homogeneous medium approximation for analysis

Biomedical Optics EXPRESS

was more reliable. More complex approaches require a detailed study of the effect of the varying upper-layer thickness due to probe pressure which is beyond the scope of this work.

It is important to note that one of the downsides of DCS is being sensitive to fiber and probe motion. For this reason its usage in dynamic, rhythmically exercise requires signal gating in order to exclude the time periods corresponding to limb movement [52–54]. We have chosen to perform an isometric exercise in order to avoid motion artifacts in DCS recording. This avoids the complications of monitoring movements and makes the experiment more feasible and easily reproducible, enlarging the possibility of applications. Also, studies suggest that repetitive static exercise (relatively short static contractions) are typical for gadget users and may decrease blood supply and prevent nutrients from being delivered to muscles, thus leading to muscle pain and fatigue [55]. On the other hands, we note that by the use of newer approaches to fast DCS methods, these limitations may be addressed in the future and the comparison of static and dynamic exercises may be enabled in a more robust manner.

Finally, we also note that we did not employ NIRS (TRS) and DCS simultaneously. This is because the fiber-optics employed by the TRS device was not suitable to be simultaneously deployed with the DCS fibers in this small tissue volume. In future, the adoption of custom TRS devices for simultaneous measurements would allow us to also estimate the metabolic rate of oxygen extraction. A follow-up study with a larger sample size would allow for a more detailed statistical analysis including a complete temporal analysis.

Following these final observations, we note another relevant application of this method. The thenar eminence area has less anatomical inter-subject variability, due to a relatively thin fat layer, making it an almost homogeneous and accessible region to NIR technologies. This muscle has been demonstrated to be a practical location to evaluate microvascular and endothelial health using NIRS derived parameters such as the muscle blood oxygen saturation in response to a vascular occlusion task (*e.g.* an arterial occlusion due to an arm cuff) as a good predictor of low central venous oxygen in septic patients [56] or readiness for ventilator weaning off process [57]. These studies (and more) are based on the idea that NIRS can measure early onsets of impairments in the peripheral circulation, *i.e.* even when systemic parameters appear in the normal range. In fact, the understanding drawn from this particular study has already been utilized in a Horizon 2020 project VASCOVID [58] where parameters derived by both DCS (BFI) and TRS (total hemoglobin concentration and muscle tissue saturation) will be combined to have a more comprehensive picture for the evaluation of endothelial and microvascular health in mechanically ventilated severe COVID-19 patients.

5. Conclusion

We have described the microvascular blood flow response in the APB during and after moderate intensity static exercise in healthy subjects. This was made possible by employing DCS, a non-invasive optical technology that allows us to continuously assess the microvascular blood flow in the muscle tissue. Since the global systemic response to exercise stress is minimized in this kind of exercise, we have monitored the local mechanism that regulates the blood perfusion to the oxygen demanding muscle. Blood flow was decreased or unchanged during 30 s of sustained isometric exercise depending on the absolute force applied. This suggested that mechanical occlusion due to increased intramuscular pressure exceeded the vasodilation consequent to the higher demand of oxygen during contraction. When the muscle was relaxed, the occlusion was opened and an increase of blood flow respect to the exercise period (and respect to baseline for low MVC group) was registered.

Funding. Fundación Cellex; Fundació Mir-Puig; Agencia Estatal de Investigación (PHOTOMETABO, PID2019-106481RB-C31/10.13039/501100011033); "Severo Ochoa" Programme for Centres of Excellence in R&D (SEV-2015-0522, CEX2019- 000910-S); "la Caixa" Foundation (LlumMedBcn); Generalitat de Catalunya (AGAUR-2017-SGR-1380,

Biomedical Optics EXPRESS

CERCA, RIS3CAT-001-P-001682 CECH); Horizon 2020 Framework Programme (101016087, 688303, 871124); FEDER/ERDF (2014/0036/2DP/2.1.1.1.0/14/APIA/VIAA/020).

Acknowledgments. This research was funded by Fundació CELLEX Barcelona, Fundació Mir-Puig, Agencia Estatal de Investigación (PHOTOMETABO, PID2019-106481RB-C31/10.13039/501100011033), the "Severo Ochoa" Programme for Centres of Excellence in R&D (SEV-2015-0522, CEX2019-000910-S), the Obra social "la Caixa" Foundation (LlumMedBcn), Generalitat de Catalunya (CERCA, AGAUR-2017-SGR-1380, RIS3CAT-001-P-001682 CECH) and European Union's Horizon 2020 programme (VASCOVID No. 101016087, LUCA No. 688303, LASERLAB-EUROPE V No. 871124), FEDER/ERDF 2014/0036/2DP/2.1.1.1.0/14/APIA/VIAA/020. We thank Hamamatsu Photonics K.K. and its Spain office for loaning the TRS-20 system and for their collaboration.

Disclosures. Turgut Durduran is an inventor on relevant patents (Patent US8082015B2, "Optical measurement of tissue blood flow, hemodynamics and oxygenation"). ICFO has equity ownership in the spin-off company HemoPhotonics S.L. Potential financial conflicts of interest and objectivity of research have been monitored by ICFO's Knowledge & Technology Transfer Department. No financial conflicts of interest were identified. Udo Weigel is the CEO, has equity ownership in HemoPhotonics S.L. and is an employee in the company.

Data availability. Data underlying the results presented in this paper are not publicly available at this time but may be obtained from the authors upon reasonable request.

References

1. D. J. Wallace, B. Michener, D. Choudhury, M. Levi, P. Fennelly, D. M. Hueber, and B. B. Barbieri, "Results of a 95-subject human clinical trial for the diagnosis of peripheral vascular disease using a near-infrared frequency domain hemoglobin spectrometer," in *Optical Tomography and Spectroscopy of Tissue III*, vol. 3597 B. Chance, R. R. Alfano, and B. J. Tromberg, eds. (1999), pp. 300–316.
2. A. Elvin, A. K. Siösteen, A. Nilsson, and E. Kosek, "Decreased muscle blood flow in fibromyalgia patients during standardised muscle exercise: A contrast media enhanced colour doppler study," Eur. J. Pain **10**(2), 137 (2006).
3. J. M. O. Arnold, J. P. Ribeiro, and W. S. Colucci, "Muscle blood flow during forearm exercise in patients with severe heart failure," Circulation **82**(2), 465–472 (1990).
4. D. P. Casey, T. B. Curry, and M. J. Joyner, "Measuring muscle blood flow: a key link between systemic and regional metabolism," Curr. Opin. Clin. Nutr. Metab. Care **11**(5), 580–586 (2008).
5. D. Sharan, M. Mohandoss, R. Ranganathan, and J. Jose, "Musculoskeletal disorders of the upper extremities due to extensive usage of hand held devices," Annals Occup. Environ. Medicine **26**(1), 22–24 (2014).
6. T. Simard and J. Roberge, "Human abductor pollicis brevis muscle "divisions" and the nerve hila," The Anat. Rec. **222**(4), 426–436 (1988).
7. M. D. Jacobson, R. Raab, B. M. Fazeli, R. A. Abrams, M. J. Botte, and R. L. Lieber, "Architectural design of the human intrinsic hand muscles," J. Hand Surg. **17**(5), 804–809 (1992).
8. E. van Oudenaarde and R. a. Oostendorp, "Functional relationship between the abductor pollicis longus and abductor pollicis brevis muscles: an EMG analysis," J. Anat. **186**(Pt 3), 509–515 (1995).
9. W. P. Cooney, K.-N. An, J. R. Daube, and L. J. Askew, "Electromyographic analysis of the thumb: a study of isometric forces in pinch and grasp," J. Hand Surg. **10**(2), 202–210 (1985).
10. F. Liu, L. Carlson, and H. K. Watson, "Quantitative abductor pollicis brevis strength testing: Reliability and normative values," J. Hand Surg. **25**(4), 752–759 (2000).
11. M. de Kraker, R. W. Selles, T. A. R. Schreuders, S. E. R. Hovius, and H. J. Stam, "The Pollexograph®: a new device for palmar abduction measurements of the thumb," J. Hand Ther. **22**(3), 271–277 (2009).
12. G. S. Phalen, "The carpal-tunnel syndrome: Seventeen years' experience in diagnosis and treatment of six hundred fifty-four hands," The J. Bone & Joint Surgery **48**(2), 211–228 (1966).
13. J. C. MacDermid and J. Wessel, "Clinical diagnosis of carpal tunnel syndrome: A systematic review," J. Hand Surg. **17**(2), 309–319 (2004).
14. H. Mathews, A. Middleton, L. Boan, M. Jacks, L. Riddick, J. Shepherd, J. Patel, A. McNeal, and S. Fritz, "Intrarater and interrater reliability of a hand-held dynamometric technique to quantify palmar thumb abduction strength in individuals with and without carpal tunnel syndrome," J. Hand Surg. **31**(4), 554–561 (2018).
15. M. I. Kulick, G. Gordillo, T. Javidi, E. S. Kilgore, and W. L. Newmeyer, "Long-term analysis of patients having surgical treatment for carpal tunnel syndrome," J. Hand Surg. **11**(1), 59–66 (1986).
16. M. Rahmani, A. R. Ghasemi Esfe, S. M. Bozorg, M. Mazloumi, O. Khalilzadeh, and H. Kahnouji, "The ultrasonographic correlates of carpal tunnel syndrome in patients with normal electrodiagnostic tests," Radiol. Med. **116**(3), 489–496 (2011).
17. E. S. Ng, K. W. Ng, and E. P. Wilder-Smith, "Provocation tests in doppler ultrasonography for carpal tunnel syndrome," Muscle & Nerve **47**(1), 116–117 (2013).
18. G. A. Vanderschueren, V. E. Meys, and R. Beekman, "Doppler sonography for the diagnosis of carpal tunnel syndrome: A critical review," Muscle & Nerve **50**(2), 159–163 (2014).
19. C. Binggeli, L. E. Spieker, R. Corti, I. Sudano, V. Stojanovic, D. Hayoz, T. F. Lüscher, and G. Noll, "Statins enhance postischemic hyperemia in the skin circulation of hypercholesterolemic patients: A monitoring test of endothelial dysfunction for clinical practice?" J. Am. Coll. Cardiol. **42**(1), 71–77 (2003).

Biomedical Optics EXPRESS

20. M. J. Joyner, N. M. Dietz, and J. T. Shepherd, "From Belfast to Mayo and beyond: the use and future of plethysmography to study blood flow in human limbs," J. Appl. Physiol. **91**(6), 2431–2441 (2001).
21. B. Grassi and V. Quaresima, "Near-infrared spectroscopy and skeletal muscle oxidative function in vivo in health and disease: a review from an exercise physiology perspective," J. Biomed. Opt. **21**(9), 091313 (2016).
22. V. Quaresima and M. Ferrari, "Functional near-infrared spectroscopy (fnirs) for assessing cerebral cortex function during human behavior in natural/social situations: a concise review," Organ. Res. Methods **22**(1), 46–68 (2019).
23. F. Scholkmann, S. Kleiser, A. J. Metz, R. Zimmermann, J. Mata Pavia, U. Wolf, and M. Wolf, "A review on continuous wave functional near-infrared spectroscopy and imaging instrumentation and methodology," NeuroImage **85**, 6–27 (2014).
24. D. A. Boas, L. E. Campbell, and A. G. Yodh, "Scattering and imaging with diffuse temporal field correlation," Phys. Rev. Lett. **75**(9), 1855–1858 (1995).
25. D. A. Boas and A. G. Yodh, "Spatially varying dynamical properties of turbid media probed with diffusing temporal light correlation," J. Opt. Soc. Am. A **14**(1), 192 (1997).
26. T. Durduran, R. Choe, W. B. Baker, and A. G. Yodh, "Diffuse optics for tissue monitoring and tomography," Rep. Prog. Phys. **73**(7), 076701 (2010).
27. G. Yu, T. F. Floyd, T. Durduran, C. Zhou, J. Wang, J. A. Detre, and A. G. Yodh, "Validation of diffuse correlation spectroscopy for muscle blood flow with concurrent arterial spin labeled perfusion MRI," Opt. Express **15**(3), 1064 (2007).
28. Y. Shang, K. Gurley, and G. Yu, "Diffuse correlation spectroscopy (DCS) for assessment of tissue blood flow in skeletal muscle: recent progress," Anat. Physiol. **3**(2), 128 (2013).
29. J. M. Gálvez, J. P. Alonso, L. A. Sangrador, and G. Navarro, "Effect of muscle mass and intensity of isometric contraction on heart rate," J. Appl. Physiol. **88**(2), 487–492 (2000).
30. B. Saltin, "Exercise hyperaemia: Magnitude and aspects on regulation in humans," J. Physiol. **583**(3), 819–823 (2007).
31. D. A. Boas, S. Sakadžic, J. Selb, P. Farzam, M. A. Franceschini, and S. A. Carp, "Establishing the diffuse correlation spectroscopy signal relationship with blood flow," Neurophotonics **3**(3), 031412 (2016).
32. M. Giovannella, D. Iba nez, C. Gregori-Pla, M. Kacprzak, G. Mitjá, G. Ruffini, and T. Durduran, "Concurrent measurement of cerebral hemodynamics and electroencephalography during transcranial direct current stimulation," Neurophotonics **5**(01), 1–12 (2018).
33. D. Contini, F. Martelli, and G. Zaccanti, "Photon migration through a turbid slab described by a model based on diffusion approximation. I. Theory," Appl. Opt. **36**(19), 4587–4599 (1997).
34. F. Martelli, S. Del Bianco, A. Ismaelli, and G. Zaccanti, *Light Propagation through Biological Tissue* (SPIE, 2010).
35. L. Dong, L. He, Y. Lin, Y. Shang, and G. Yu, "Simultaneously extracting multiple parameters via fitting one single autocorrelation function curve in diffuse correlation spectroscopy," IEEE Trans. Biomed. Eng. **60**(2), 361–368 (2013).
36. R. Core Team, "R: A Language and Environment for Statistical Computing," (2016).
37. S. J. Matcher, M. Cope and, and D. T. Delpy, "In vivo measurements of the wavelength dependence of tissue-scattering coefficients between 760 and 900 nm measured with time-resolved spectroscopy," Appl. Opt. **36**(1), 386–396 (1997).
38. P. Taroni, A. Pifferi, A. Torricelli, D. Comelli and, and R. Cubeddu, "In vivo absorption and scattering spectroscopy of biological tissues," The royal society Chem. **2**(2), 124–129 (2003).
39. I. Piorvano, S. Porcelli, F. Azzarello, R. Re, L. Spinelli, D. Contini, M. Marzorati and, and A. Torricelli, "Preliminary vastus lateralis characterization with time domain near infrared spectroscopy during incremental cycle exercise," Proc. SPIE **11074**, 1107424 (2019).
40. A. Torricelli, A. Pifferi, V. Quaresima, A. Pifferi, G. Biscotti, L. Spinelli, P. Taroni, M. Ferrari and, and R. Cubeddu, "Mapping of calf muscle oxygenation and haemoglobin content during dynamic plantar flexion exercise by multi-channel time-resolved near-infrared spectroscopy," Phys. Med. Biol. **49**(5), 685–699 (2004).
41. F. Liu, H. K. Watson, L. Carlson, I. Lown, and R. Wollstein, "Use of quantitative abductor pollicis brevis strength testing in patients with carpal tunnel syndrome," Plast. Reconstr. Surg. **119**(4), 1277–1283 (2007).
42. H. Gangata, R. Ndou, and G. Louw, "The contribution of the palmaris longus muscle to the strength of thumb abduction," Clinical Anatomy **23**(4), 431–436 (2010).
43. R. H. Fitts, K. S. McDonald, and J. M. Schluter, "The determinants of skeletal muscle force and power: Their adaptability with changes in activity pattern," J. Biomech. **24**(Suppl. 1), 111–122 (1991).
44. V. F. Gladwell and J. H. Coote, "Heart rate at the onset of muscle contraction and during passive muscle stretch in humans: A role for mechanoreceptors," J. Physiol. **540**(3), 1095–1102 (2002).
45. Y. Hellsten, M. Nyberg, L. G. Jensen, and S. P. Mortensen, "Vasodilator interactions in skeletal muscle blood flow regulation," J. Physiol. **590**(24), 6297–6305 (2012).
46. F. A. Gaffney, G. Sjoegaard, and B. Saltin, "Cardiovascular and metabolic responses to static contraction in man," Acta Physiol. Scand. **138**(3), 249–258 (1990).
47. D. M. Wigmore, B. M. Damon, D. M. Pober, and J. A. Kent-Braun, "MRI measures of perfusion-related changes in human skeletal muscle during progressive contractions," J. Appl. Physiol. **97**(6), 2385–2394 (2004).
48. C. J. McNeil, M. D. Allen, E. Olympico, J. K. Shoemaker, and C. L. Rice, "Blood flow and muscle oxygenation during low, moderate, and maximal sustained isometric contractions," Am. J. Physiol. - Regul. Integr. Comp. Physiol. **309**(5), R475–R481 (2015).

Biomedical Optics EXPRESS

49. M. S. Laaksonen, K. K. Kalliokoski, H. Kyröläinen, J. Kemppainen, M. Teräs, H. Sipilä, P. Nuutila, and J. Knuuti, "Skeletal muscle blood flow and flow heterogeneity during dynamic and isometric exercise in humans," Am. J. Physiol. - Hear. Circ. Physiol. **284**(3), H979–H986 (2003).
50. H. Degens, S. Salmons, and J. C. Jarvis, "Intramuscular pressure, force and blood flow in rabbit tibialis anterior muscles during single and repetitive contractions," Eur. J. Appl. Physiol. Occup. Physiol. **78**(1), 13–19 (1998).
51. T. Osada, S. P. Mortensen, and G. Rådegran, "Mechanical compression during repeated sustained isometric muscle contractions and hyperemic recovery in healthy young males," J. Physiol. Anthropol. **34**(1), 36 (2015).
52. Y. Shang, T. B. Symons, T. Durduran, A. G. Yodh, and G. Yu, "Effects of muscle fiber motion on diffuse correlation spectroscopy blood flow measurements during exercise," Biomed. Opt. Express **1**(2), 500–511 (2010).
53. K. Gurley, Y. Shang, and G. Yu, "Noninvasive optical quantification of absolute blood flow, blood oxygenation, and oxygen consumption rate in exercising skeletal muscle," J. Biomed. Opt. **17**(7), 0750101 (2012).
54. V. Quaresima, P. Farzam, P. Anderson, P. Y. Farzam, D. Wiese, S. A. Carp, M. Ferrari, and M. A. Franceschini, "Diffuse correlation spectroscopy and frequency-domain near-infrared spectroscopy for measuring microvascular blood flow in dynamically exercising human muscles," J. Appl. Physiol. **127**(5), 1328–1337 (2019).
55. N. L. Radwan, M. M. Ibrahim, and W. S. E. Mahmoud, "Evaluating hand performance and strength in children with high rates of smartphone usage: an observational study," J. Phys. Ther. Sci. **32**(1), 65–71 (2020).
56. J. Mesquida, J. Masip, G. Gili, A. Artigas, and F. Baigorri, "Thenar oxygen saturation measured by near infrared spectroscopy as a noninvasive predictor of low central venous oxygen saturation in septic patients," Intensive Care Med. **35**(6), 1106–1109 (2009).
57. G. Gruartmoner, J. Mesquida, J. Masip, M. L. Martínez, A. Villagra, F. Baigorri, M. R. Pinsky, and A. Artigas, "Thenar oxygen saturation during weaning from mechanical ventilation: an observational study," Eur. Respir. J. **43**(1), 213–220 (2014).
58. Portable platform for the assessment of microvascular health in COVID-19 patients at the intensive care, https://vascovid.eu/.